ORNL/TM-2022/2765
CRADA/NFE-16-06257

CRADA Final Report: High-Efficiency Thermoelectric Clothes Dryer

Kyle R. Gluesenkamp
Philip R. Boudreaux
Viral K. Patel
Guolian Wu
Ravee Vaidhyanathan

May 2024

OAK RIDGE
National Laboratory

ORNL/TM-2022-2765
CRADA/NFE-16-06257

Buildings and Transportation Science Division

CRADA FINAL REPORT: HIGH-EFFICIENCY THERMOELECTRIC CLOTHES DRYER

Kyle R. Gluesenkamp[1]
Philip R. Boudreaux[1]
Viral K. Patel[1]
Guolian Wu[2]
Ravee Vaidhyanathan[2]

[1] Buildings and Transportation Science Division, ORNL
[2] Samsung Electronics America (SEA)

May 2024

Prepared by
OAK RIDGE NATIONAL LABORATORY
Oak Ridge, Tennessee 37831-6283
managed by
UT-BATTELLE, LLC
for the
US DEPARTMENT OF ENERGY
under contract DE-AC05-00OR22725

CONTENTS

LIST OF FIGURES

LIST OF TABLES

NOMENCLATURE

BTO	Building Technologies Office
CEF	combined energy factor
CRADA	Cooperative Research and Development Agreement
DOE	US Department of Energy
GWP	global warming potential
HX	heat exchanger
OEM	original equipment manufacturer
ORNL	Oak Ridge National Laboratory
SEA	Samsung Electronics America
TE	thermoelectric
TED	thermoelectric [clothes] dryer
TEHP	thermoelectric heat pump

ABSTRACT

A typical clothes dryer in the United States accounts for 7% of the average residential customer's electric bill. Nationwide, consumers pay about $9 billion annually for clothes drying. Although energy efficiency for most household appliances has improved by a factor of two or more in recent decades, today's clothes dryers perform similarly to units from the 1970s. Dryer efficiency is measured by the combined energy factor (CEF), and today's units typically dry 3.73 lb of cloth per kilowatt-hour consumed. An ENERGY STAR–qualified unit must achieve 3.93 lb/kWh (for standard-size electric units) and dry in less than 80 min.

Oak Ridge National Laboratory (ORNL) and CRADA partner Samsung Electronics America have developed an efficient prototype clothes dryer that uses thermoelectric heat pumps instead of electric resistance to dry the clothes. The prototype fabricated at ORNL successfully demonstrated in the laboratory a CEF of 6.89 lb/kWh at standard conditions of 75°F and 50% relative humidity (RH), exceeding the original project target of 6.0 lb/kWh. Additional trials on the same prototype achieved faster dry times with slightly lower CEFs, meeting all requirements for ENERGY STAR product qualification. Deploying dryers with CEFs of 6.0 lb/kWh nationwide represents a technical potential of 234 TBtu/year primary energy savings. The modeling and prototype development activities for the thermoelectric clothes dryer under this CRADA are summarized in this final report.

1. STATEMENT OF OBJECTIVES

The goal of this effort was to perform a design and evaluation study to determine the feasibility of introducing a residential thermoelectric clothes dryer (TED) at a cost that would enable mass market adoption in the United States. Research and development were conducted to evaluate the technical and commercial viability of solid-state thermoelectric heat pump (TEHP) clothes dryer technology to improve efficiency levels, reduce emission levels, and avoid the use of refrigerants with global warming potential (GWP).

2. BENEFITS TO THE BUILDING TECHNOLOGIES OFFICE MISSION

In its 2020 multiyear program plan, the US Department of Energy's (DOE) Building Technologies Office (BTO) set a target to introduce clothes dryer technologies with 50% reduction in energy consumption compared with conventional models and with an installed cost premium per unit of less than $565 (DOE 2016). In addition, the BTO specifically sought advanced non–vapor compression heat pump solutions to facilitate phase-out of GWP refrigerants from widespread use. Work for this Cooperative Research and Development Agreement (CRADA) directly addressed these needs.

Dryers using vapor compression heat pumps have been commercialized and recently entered the US retail market. However, those dryers utilize refrigerants with significant GWPs and are typically sold at price premiums of over $1,100 compared with base efficiency models.

In this project, a TED suitable for the current US retail market was designed, prototypes were produced for lab testing, and the performance of the prototypes was evaluated. Evaluation showed that this zero-GWP, non–vapor compression, high-efficiency TED achieves DOE BTO goals.

3. TECHNICAL DISCUSSION OF WORK PERFORMED BY ALL PARTIES

Work for the CRADA involved the development and testing of two TED prototypes, which was a continuation of previous work by Oak Ridge National Laboratory (ORNL). The first prototype under the CRADA (2b) involved testing a new heat exchanger (HX) used to transfer heat from the thermoelectric (TE) modules to the air. The third-generation TED involved iterations of a new TEHP that used a pumped water loop with tube-and-fin water-to-air HXs instead of using the heat sinks for heat transfer as in Generation 2b. All generations of the TED, both before and during the CRADA, are outlined in Table 1. This report focuses on describing the work performed for Generations 2b–3d TED prototype development.

Table 1. Overview of prototype generations

Prototype generation and notes	Funding source	System	HX used	TE module type and count	Key lessons learned
Gen 1	BENEFIT FOA[a]		Direct contact	Electric resistance	Surface contact alone does not provide sufficient heat transfer
Gen 2a	BENEFIT FOA		Pin fins, air to TE	36 TE modules with 199 couples each, 40 × 40 mm each, provided by Sheetak (see Figure 1)	Mass and cost of Al are far too high using this HX geometry
Gen 2b	CRADA project		Extruded fins, air to TE	144 TE modules (36 groups of 4) with 51 couples each, supplied by Sheetak. Then later on the same system, 144 TE modules (36 groups of 4) with 71 couples each, supplied by Sheetak	Mass and cost of Al are still high using extruded fins; also, manufacturing difficulties are expected because of the large number of mating surfaces
Gen 3a	CRADA project		Microchannels with plastic headers	20–30 TE modules, supplied by Thermonamic	Al microchannels with plastic headers leak at interface

Table 1. Overview of prototype generations (continued)

Prototype generation and notes	Funding source	System	HX used	TE module type and count	Key lessons learned
Gen 3b	CRADA project		Microchannels with Al headers + ability to use six banks of five TE modules in TEHP	20–30 TE modules, supplied by Thermonamic	No marked improvement in efficiency over 3a; however, a marked improvement in durability using new Al headers was observed
Gen 3c	CRADA project		Redesigned water-to-air HXs	20–30 TE modules, supplied by Thermonamic	New HXs increased the combined energy factor by 0.3 and decreased dry time by ~ 8 min
Gen 3d	CRADA project		High-efficiency blower and drum motor	20–30 TE modules, supplied by Thermonamic	Simple component swaps with a more efficient blower and drum motor showed higher performance, but these components would increase cost. Observed that the current profile applied to the TE modules throughout the test can greatly affect the performance

[a] Buildings Energy Efficiency Frontiers & Innovation Technologies Funding Opportunity Announcement

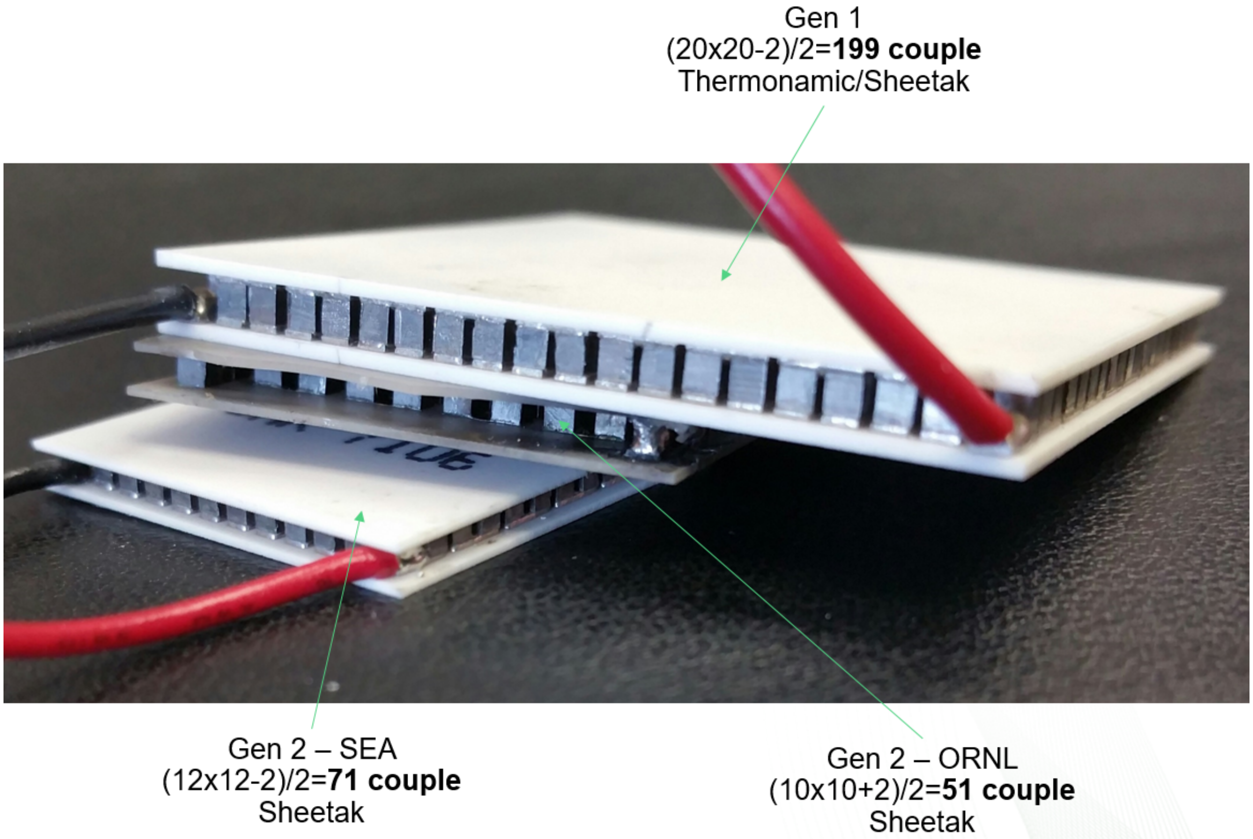

Figure 1. TE module comparison used in different TED prototypes.

3.1 TEST FACILITY AND EXPERIMENTAL MEASUREMENT METHODOLOGY

3.2 COMBINED ENERGY FACTOR MEASUREMENT

Tests to measure the combined energy factors (CEFs) of all dryer prototypes in this work were conducted according to the Code of Federal Regulations (10 CFR Part 430). This enabled comparison with current clothes dryers on the market. During the CRADA work, the minimum CEF was 3.73 lb_c/kWh (pounds of cloth per kilowatt-hour) for a standard load of fabric in the United States for a standard vented electric clothes dryer.

3.3 SECOND-GENERATION PROTOTYPE (2b)

The second-generation (2b) TED prototype was the first prototype tested at the beginning of the CRADA period. More details can be found in the published journal article describing the experimental performance of this prototype (Patel, Gluesenkamp, Goodman, and Gehl 2018). This prototype (shown in Figure 2) used 144 TE modules with extruded fin heat sinks to transfer heat to and from the TE modules and air. The dryer had an open-airflow path, with air flowing through components in the following order: blower, TE module hot side, drum, filter, TE module cold side, exhaust. The TEHP was driven electrically with 3 separate banks of TE modules, with 48 TE modules in each bank. CEF tests were completed in which the total energy consumption was calculated as shown in Eq. (1),

$$E\ (W) = \left(\frac{t}{3{,}600}\right) \times \left(\frac{P_{Te}}{\eta_{PS}} + P_{drum} + P_{blower}\right), \#(1)$$

where t is the dry time in seconds, P_{TE} is the average DC power consumption of the TE modules during the test, η_{PS} is the AC to DC conversion efficiency of the TE power supplies, and P_{drum} and P_{blower} are the average power consumption of the drum rotation motor and blower, respectively.

Figure 2. TED Generation 2b (left) with TEHP at the bottom (right).

Experiments were conducted with varying currents applied to the different TE banks. Table 2 shows the results from these trials. Comparing Trial 4 with Trials 2 and 3, both the dry time and CEF improved as more current was applied to the TE modules. Additionally, comparing Trial 1 with the other trials, at lower airflow rates and lower TE currents, the dry time increased while the CEF improved.

Table 2. Experimental CEF test results for Generation 2b TED

	Airflow rate (cfm)	Current applied (A)			Dry time (min)	CEF (lb_c/kWh)
		Bank 1	Bank 2	Bank 3		
Trial 1	123	1.18	1.24	1.31	158.7	6.51
Trial 2	138	1.40	1.90	2.40	107.4	5.36
Trial 3	140	1.40	1.90	2.40	100.1	5.48
Trial 4	141	2.00	2.00	2.00	96.1	5.60

The Generation 2b prototype was also built at Samsung for further testing.

3.4 THIRD-GENERATION PROTOTYPE

The Generation 3 prototype TED differed from previous generations by the addition of an intermediate hydronic loop to transfer heat from the hot side of the TE modules to the air used to dry the cloth. The appliance schematic is shown on the left side of Figure 3. Notice both hot and cold water-to-air HXs in line with the airflow. The hot HX was located before the drum for heating the incoming air, and the cold HX was located after the drum and was used as the heat source for the TE modules. The left side of Figure 4 shows the hydronic loops connecting the hot and cold water-to-air HXs to the hot and cold sides of the TE modules, respectively. The complete air circuit consisted of the following components beginning from the air inlet from inside the cabinet to the exhaust: a hot water-to-air HX, an electric resistance heater, a drum, a filter, a blower, a cold water-to-air HX, an airflow measurement station with an air straightener, and an auxiliary axial blower that vented to the ambient environment.

To demonstrate the Generation 3 prototype, the right side of Figure 4 shows the two banks of TE modules, and Figure 5 shows the entire TEHP incorporated into the clothes dryer. Five TE modules were powered serially in each bank with a constant-current power supply. The TE modules were thermally connected using graphite paper or Arctic Silver thermal paste to two Al channels which water flowed through, one on the hot side of the TE modules and one on the cold side (Figure 5, left). The Al microchannels had acrylonitrile butadiene styrene plastic headers with nipples so that four–six banks (of five TE modules each) could be connected to form a hydronic loop for the TEHP. Figure 5 shows the TEHP used for the first tests of the Generation 3 prototype with five banks of TEs.

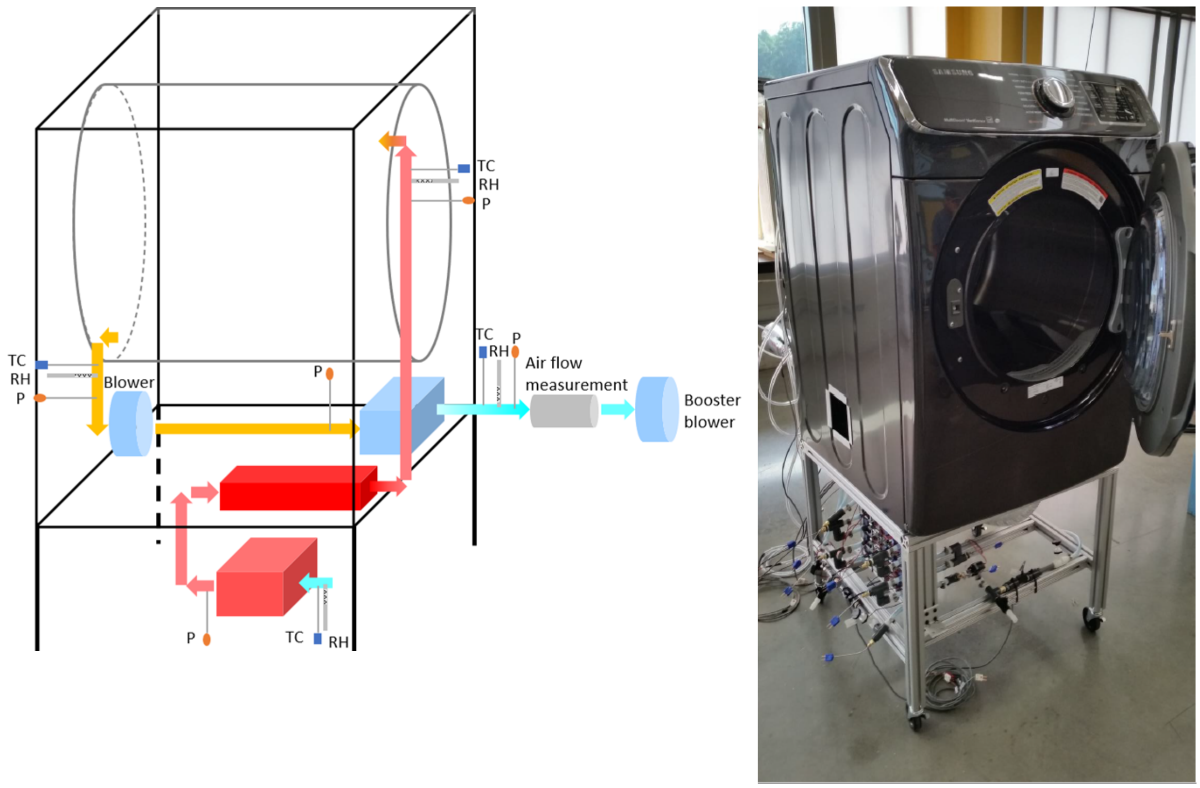

Figure 3. Schematic of components used in Generation 3 of the TED (left) and image of the fabricated Generation 3 prototype of the TED (right).

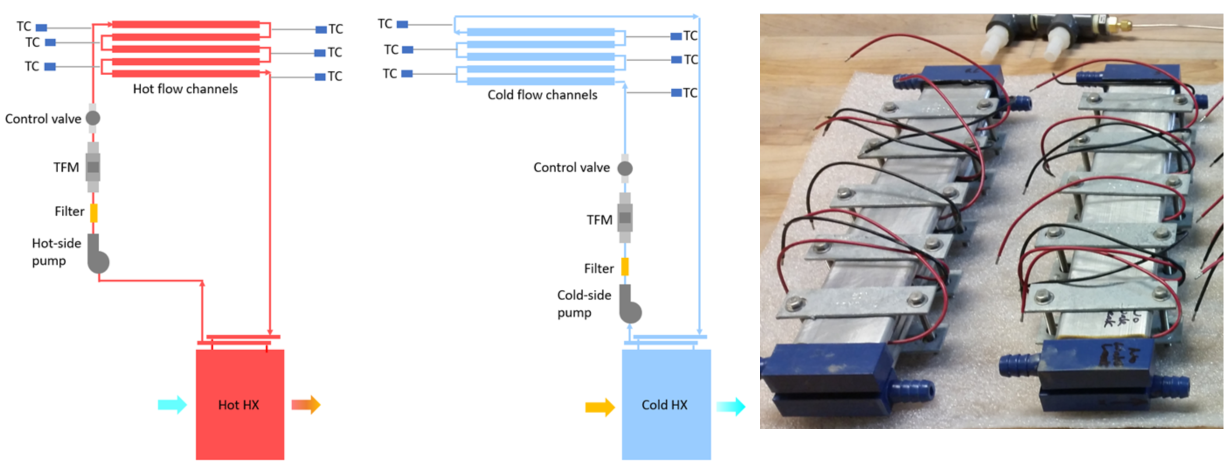

Figure 4. Schematic of the hot and cold water loops (left) and TE and water microchannel assemblies, with five TE modules used in each of the two banks shown (right). Aluminum microchannels were used on both the top (hot side) and bottom (cold side) of the TE modules. Blue headers with nipples on the microchannels were used for connection to other TE banks or components of the water loops. A total of 5 banks (25 TE modules) were used for the Generation 3 TED prototype.

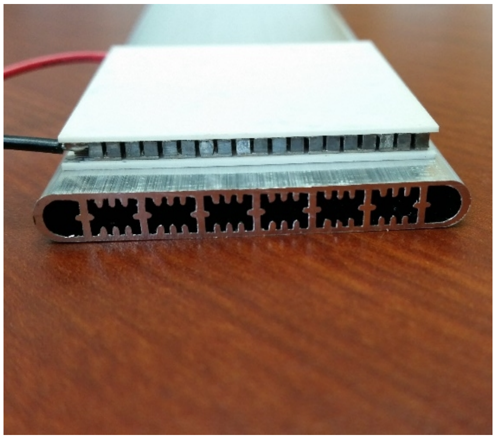

Figure 5. Image showing the internal structure of the Al microchannels with TE module on top (left) and image of the TEHP (right). Five banks of five TE models were connected in series to heat water that in turn heated the inlet air of the dryer via a water-to-air HX.

3.4.1 Experimental Results and Design Changes

The TED Generation 3 prototype underwent four major hardware iterations through the experimental testing period as shown in Figure 6:

1. Initial design
2. Redesigned microchannel headers
3. Redesigned water-to-air HXs
4. Installation of an efficient blower and dedicated drum rotation motor

Experimental trials using the procedure outlined in Appendix D1, "Uniform Test Method for Measuring the Energy Consumption of Clothes Dryers," of 10 CFR 430, Subpart B, were completed between September 2017 and January 2020 (10 CFR Part 430). In comparison with the initial prototype performance, the new blower and rotation motor showed the biggest improvements in CEF. The other major contributor to efficiency was the adjustment of TE current, which does not fall into the hardware change category.

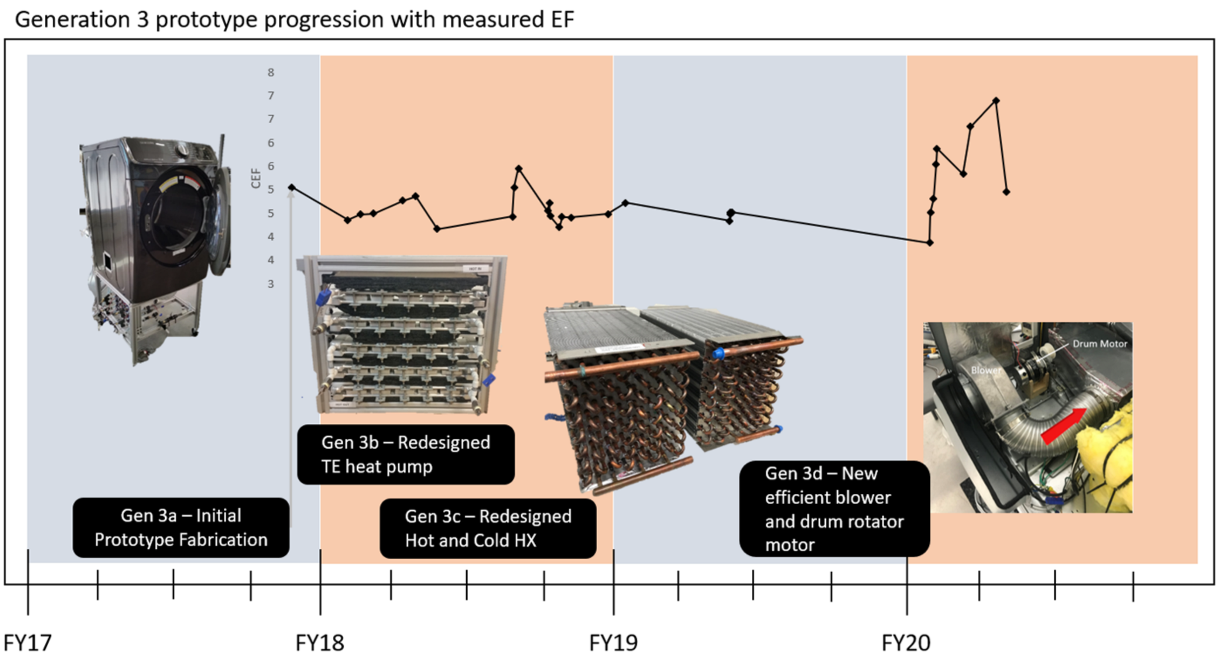

Figure 6. Hardware changes during Generation 3 of the TED prototype. CEF trace shows the performance of all trials with an 8.45 lb DOE load.

After prototype fabrication of the Generation 3 unit was finished, 10 CEF trials were completed with the TED before any hardware changes were made. Figure 7 shows the dry time and CEF of each trial, and Table 3 shows details of each trial including load size and applied TE current. Performance differed from Trial 9 to Trial 10, illustrating that lower TE current resulted in higher efficiency but longer dry time.

The difference in performance of Trials 2, 3, 6, and 7 show system variability, as all these trials were under the same control conditions: load size and TE current. Trial 7 did have the hot air duct insulated, unlike the previous trials, which could have contributed to it being the best-performing trial of this four-trial group.

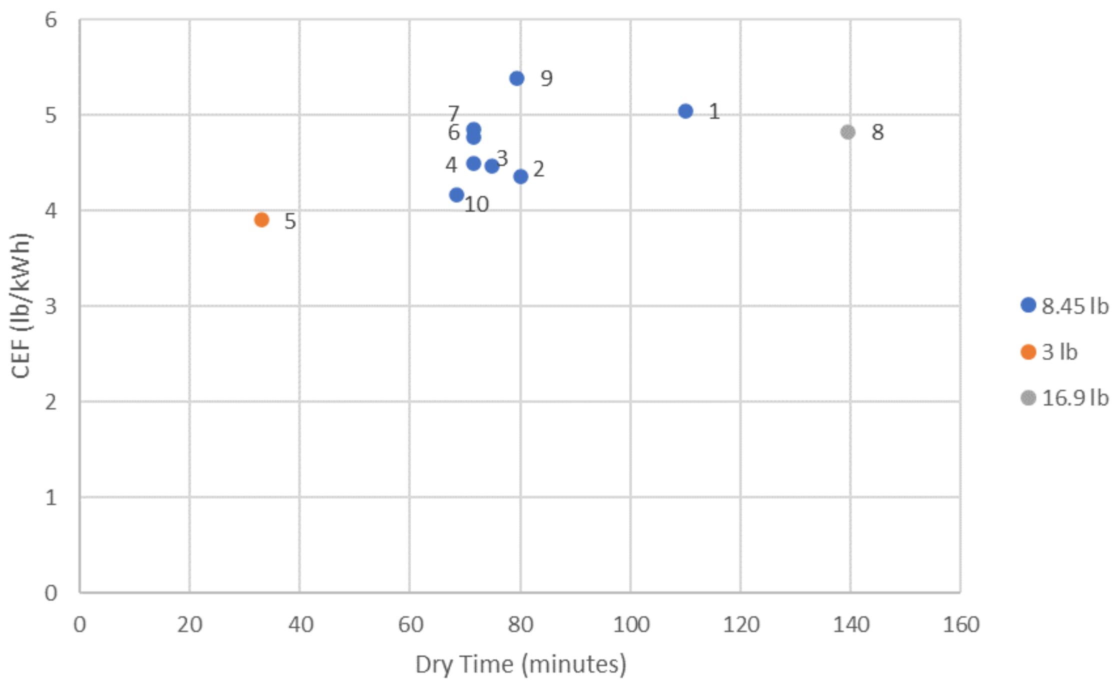

Figure 7. CEF trial results using the initial Generation 3 prototype design (Generation 3a). The number by each dot indicates the corresponding trial.

Table 3. CEF trial details of the initial prototype (Generation 3a)

Trial #	Load size (lb)	Airflow rate (cfm)	TE current (A)	Dry time (min)	CEF (lb_c/kWh)	Notes
1	8.45		3	110	5.05	
2	8.45		4	80	4.36	
3	8.45	127	4	75	4.47	
4	8.45	129	4	71.6	4.49	Ran 300 W electric resistance heat for first 30 min of cycle
5	3.00	145	4	33	3.91	
6	8.45	142	4	71.5	4.77	
7	8.45	144	4	71.6	4.86	Insulation on air duct between hot HX and drum
8	16.90	140	4	139.6	4.83	Cold side manifold started leaking
9	8.45	144	3.5	79.5	5.40	
10	8.45	145	4.5	68.6	4.17	Major water leak on hot side manifold

3.4.1.1 Design Change 1 (Generation 3b) – Redesigned TEHP

The first major hardware change to the Generation 3 prototype was to address water leaks in the initial TEHP design. The plastic headers glued to the Al microchannels started cracking and leaking after numerous drying cycles. To address this, Al headers were fashioned that were welded to the microchannels as shown on the left side of Figure 8. Instead of barb fittings, these Al headers utilized straight Al tubing so that push-to-connect fittings could be utilized. This change enabled up to six banks of five TE modules to be connected if needed.

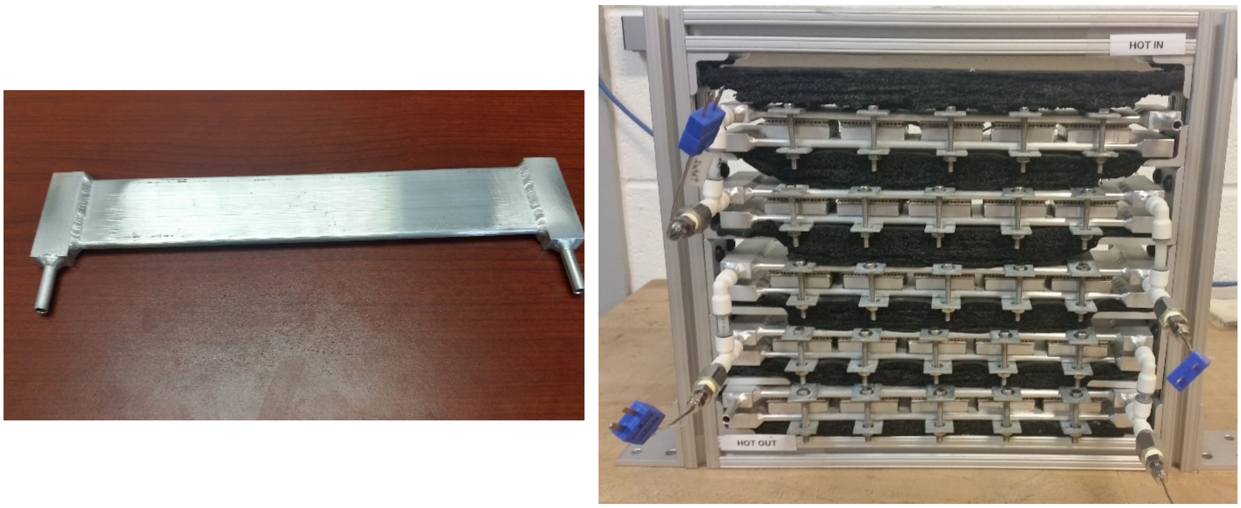

Figure 8. Aluminum headers welded onto the microchannels to ensure water did not leak out of the hydronic loops (left) and TEHP reassembled with new Al headers and push-to-connect fittings (right).

Figure 9 and Table 4 show the performance and details of the CEF trials after the TEHP was repaired. The main parameter that was changed across these three trials was the TE current; again, as the current was reduced, the trials were more energy efficient but took longer. In comparison with trials completed for Generation 3a, no marked improvement was observed after the TEHP repair.

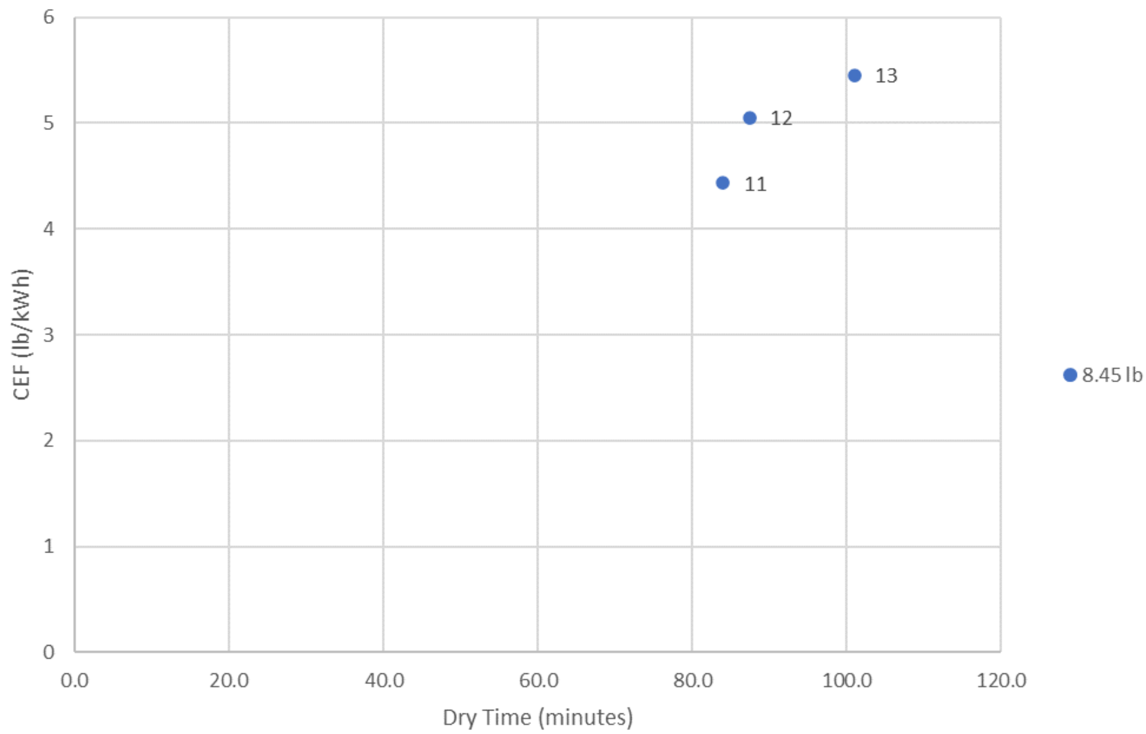

Figure 9. CEFs of trials after TEHP repair (Generation 3b). The number by each dot indicates the corresponding trial.

Table 4. CEF trial details after TEHP repair (Generation 3b)

Trial #	Load size (lb)	Airflow rate (cfm)	TE current (A)	Dry time (min)	CEF (lb_c/kWh)
11	8.45	148	4.0	84.0	4.43
12	8.45	136	3.5	87.4	5.05
13	8.45	135	3.0	101.1	5.45

3.4.1.2 Design Change 2 (Generation 3c) – Redesigned water-to-air HXs

Neither of the original water-to-air HXs performed to design expectations. The cold water-to-air HX had an air-side pressure drop 17% higher than the design target, and the hot HX did not meet the designed approach temperature. Table 5 shows the designed and measured performance of the original and redesigned HXs. The original hot and cold HXs were both swapped for the redesigned HXs. Figure 10 shows pictures of the new hot water-to-air HX compared with the original.

Table 5. Design parameters and measured performance of original and newly designed hot and cold water-to-air HXs

		Hot HX – V1	Hot HX – V2 (Redesigned)	Notes
Pressure drop (ΔP), air side	ΔP target	<0.4 in. WC	<0.4 in. WC	
	ΔP design	0.26 in. WC @ 150 cfm	0.15 in. WC @ 104 cfm	Super Radiator's calculator
	ΔP measured	0.1 in. WC @ 93 cfm-in / 104 cfm-out	0.17 in. WC @ 100 cfm-in / 111 cfm-out	
Approach temperature (AT)	AT target	Fluid in – air out <5 K		
	AT design	55°C – 44°C = 11 K	71.7°C – 68.8°C = 3 K	
	AT measured	Thtw6-Thxao 71.7°C – 62.6°C = 9.1 K	Thtw6-Thxao 72.4°C – 61.4°C = 11.0 K	@ 40 min into test
		Cold HX – V1	**Cold HX – V2 (Redesigned)**	**Notes**
ΔP (air side)	ΔP target	<0.4 in. WC	<0.4 in. WC	
	ΔP design	0.26 in. WC @ 150 cfm	0.15 in. WC @ 138 cfm	
	ΔP measured	0.47 in. WC @ 151 cfm-in / 138 cfm-out	0.39 in. WC @ 158 cfm-in / 144 cfm-out	
AT	AT target	Air out – fluid in <5 K		
	AT design	18.7 – 14°C = 4.7 K	22 – 17.5°C = 4.5 K	
	AT measured	Tcxao-Tctw6 24.3 – 19.8°C = 4.5 K	Tcxao-Tctw6 22.2 – 17.7°C = 4.5 K	

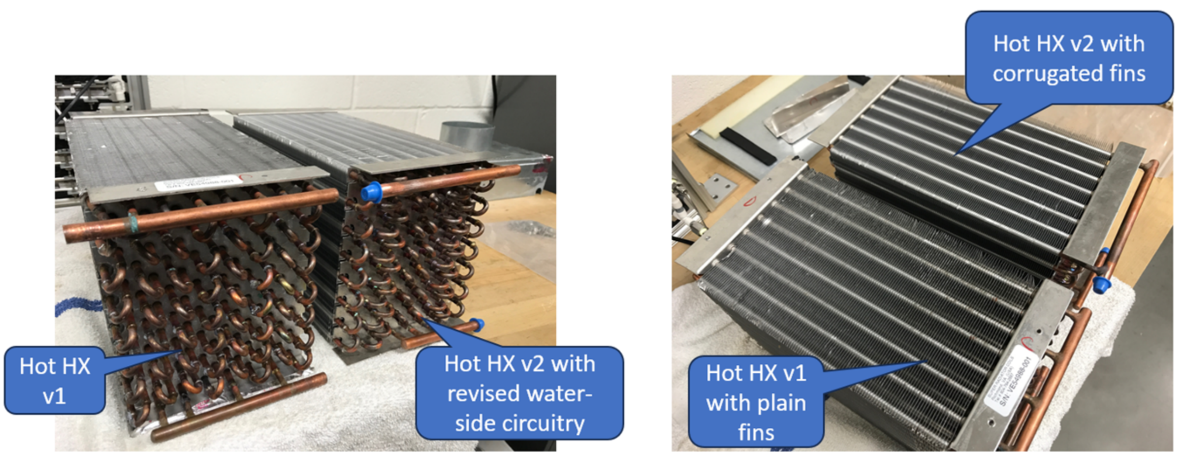

Figure 10. Comparison of newly designed hot water-to-air HX to original.

Figure 11 and Table 6 show dryer performance trials completed after the new HXs were installed. The variation in performance between Trials 21 and 25 was mainly due to the different current-control schemes of the TE modules. Trial 21 can be compared with Trial 11 to determine any improvement the newly redesigned HXs might have had on performance. Trial 11 had a CEF of 4.4 lb_c/kWh and a dry time of 84 min, and Trial 21 had a CEF of 4.7 lb_c/kWh with a dry time of 76.2 min, so some improvement was made by replacing the HXs with the redesigned ones.

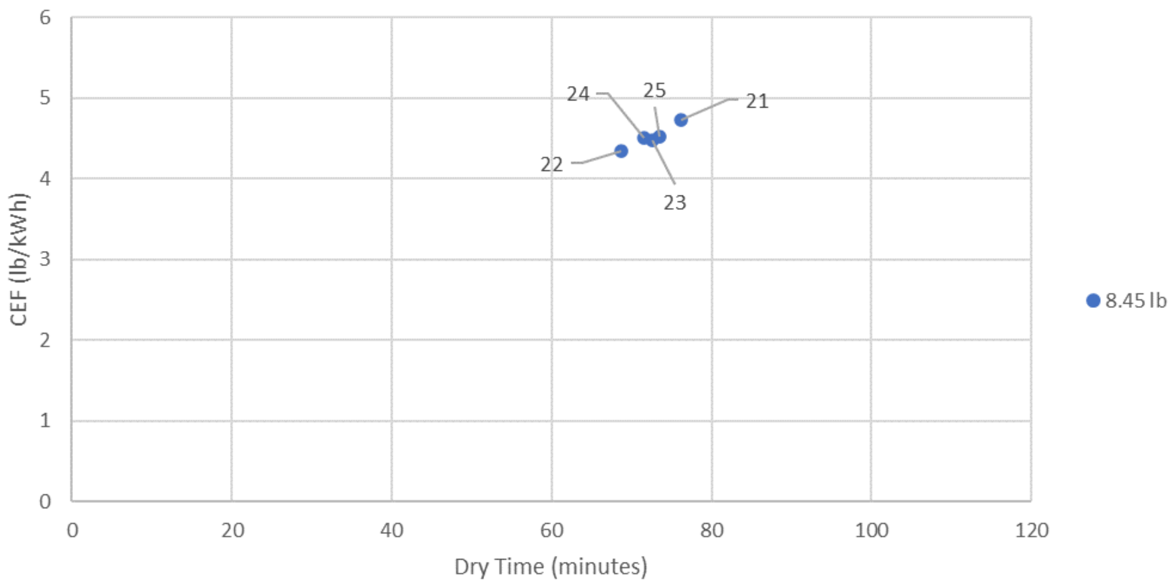

Figure 11. CEFs of trials after newly designed HXs were installed (Generation 3c). The number by each dot indicates the corresponding trial.

Table 6. CEF trial details after newly redesigned HXs were installed (Generation 3c)

Trial #	Load size (lb)	Airflow rate (cfm)	TE current (A)	Dry time (min)	CEF (lb_c/kWh)	Notes
21	8.45	155.7	4.0	76.2	4.72	5 TE banks
22	8.45	158.5	5.0	68.7	4.34	4 TE banks
23	8.45	151.5	4.5/5.0	72.6	4.48	4 TE banks: 4.5 A applied to 2, 5 A applied to 2
24	8.45	149.8	4.5/5.0	71.48	4.51	4 TE banks: 4.5 A applied to 2, 5 A applied to 2
25	8.45	149.7	4.0–5.6	73.5	4.53	4 TE banks: 4–5.6 A applied to each bank.

3.4.1.3 Design Change 3 (Generation 3d) – New high-efficiency blower and drum rotator motor

The original equipment manufacturer (OEM) motor had an impeller for airflow on one side of the motor and a pulley to turn the drum on the other side of the motor. The average motor wattage used for moving air was approximately 174 W to provide 147 cfm at 0.9 Pa of fan head for a static fan efficiency of 9%. The static fan efficiency was calculated using Eq. (2),

$$\eta_s = \frac{\Delta p_s \times V}{P} \#(2)$$

where Δp_s is the fan head in pascals, V is the volumetric flow rate in meters per second, and P is the power consumption of the fan in watts. An ebm-papst centrifugal fan (model G3G146-AB72-01) was installed in place of the OEM motor, and a DC motor was used to rotate the drum. Figure 12 compares the performance of the ebm blower with that of the stock blower. For a particular fan head, the ebm blower provided increased airflow over the OEM blower. During normal TED operation, the ebm blower with the auxiliary blower enabled 170 cfm of air to flow through the system, whereas with the OEM blower plus auxiliary blower, the TED was capable of only 140 cfm. Figure 13 shows the new parts installed in the base of the dryer compared with the OEM parts.

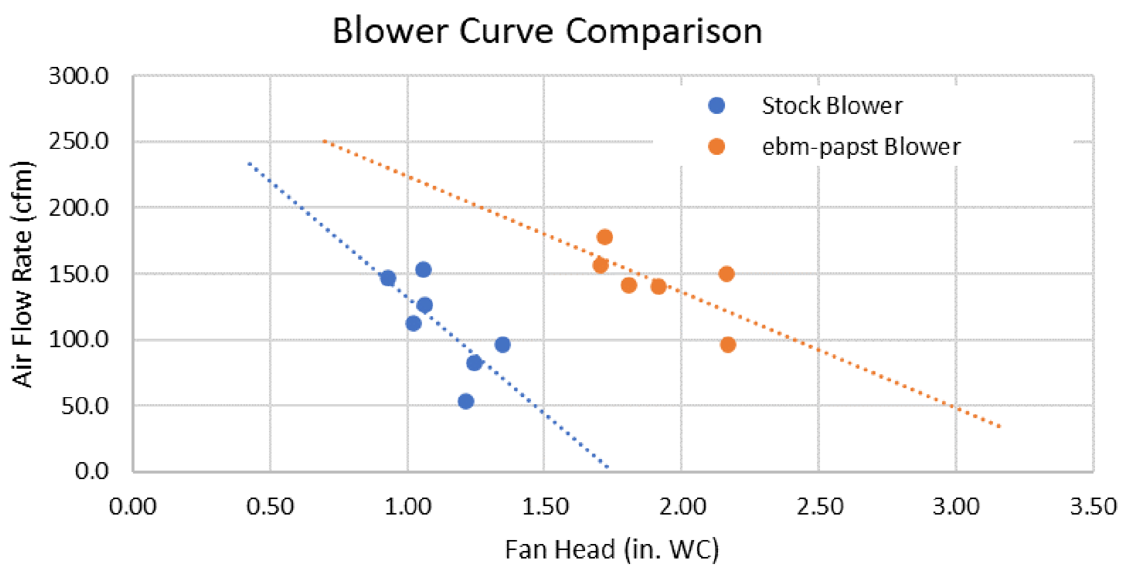

Figure 12. Measured performance of the stock and ebm blowers.

Figure 13. OEM blower and drum rotation pulley connected to one motor (left) and ebm blower and dedicated drum rotation motor fit into the same footprint as the OEM parts (right). Red arrow shows direction of airflow.

Figure 14 and **Error! Reference source not found.** describe the experimental results after changing the blower and rotator motor in the dryer. The increased airflow and higher efficiency from the new blower enabled more efficient operation of the dryer. At 4 A for an 8.45 lb load, the dryer had a CEF of 4.72 before the new blower (Trial 21) and a CEF of 5.55 after the new blower install (Trial 29). However, as other trials suggested, running the TE modules at lower currents markedly increased efficiency. Trial 33, in which the TE modules were driven at 3 A, yielded a CEF of 6.89 for an 8.45 lb load. However, running at a lower current increased the drying time by about 20 min. Trials 29 and 33 met the project performance targets for normal and eco-mode drying, respectively.

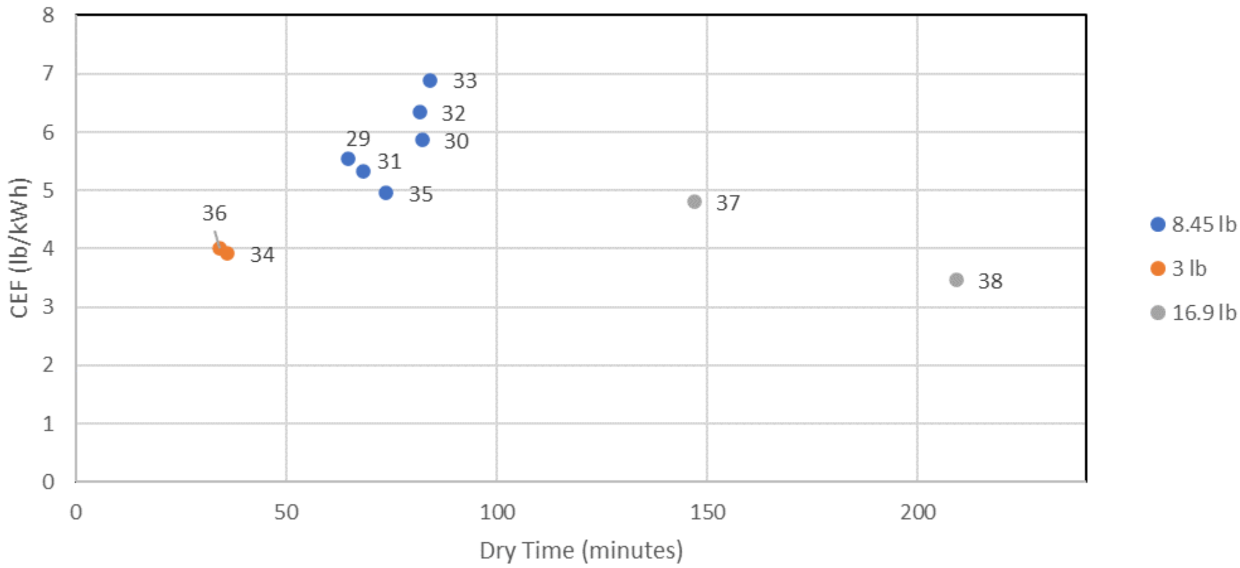

Figure 14. Performance results of trials for Generation 3d. The number by each dot indicates the corresponding trial.

Table 7. Trial details for Generation 3d

Trial #	Load size (lb)	Airflow rate (cfm)	TE current (A)	Dry time (min)	CEF (lb_c/kWh)	Notes
29	8.45	176	4.0	64.6	5.55	5 TE banks
30	8.45	176	3.3	82.4	5.87	
31	8.45	166	4.0	68.33	5.33	Reduced leakage between drum and blower inlet
32	8.45	167	4.0	81.73	6.34	2 banks lost power for most of test, resulting in very high EF
33	8.45	165	3.0	84.32	6.89	
34	3.00	166	4.0	36.08	3.92	
35	8.45	163	4.0	73.8	4.96	
36	3.00	169	4.0	34.17	4.01	
37	16.9	174	4.0	146.98	4.81	
38	16.9	172	4.0	209.17	3.47	

4. SUBJECT INVENTIONS (AS DEFINED IN THE CRADA)

Significant advances were made in the state of the art of the technology in this CRADA. However, the existence of significant related prior art prevented the submission of a patent application for the water-based design.

5. DISSEMINATION AND COMMUNICATIONS

5.1 JOURNAL PAPERS

Boudreaux, P., Gluesenkamp, K. R., Patel, V. K., Shen, B. 2020. "Measurement and Analysis of Clothes Dryer Air Leakage." *Drying Technology*, vol. 39, no. 14, 2105–2117, https://doi.org/10.1080/07373937.2020.1753765.

Gluesenkamp, K. R., Boudreaux, P., Patel, V., Goodman, D., Shen, B. 2019. "An Efficient Correlation for Heat and Mass Transfer Effectiveness in Tumble-Type Clothes Dryer Drums." *Energy*, vol. 172, 1225–1242.

Gluesenkamp, K. R., Patel, V. K., Momen, A. M. 2020. "Efficiency Limits of Evaporative Fabric Drying Methods." *Drying Technology*, vol. 39, no. 1, 104-124, https://doi.org/10.1080/07373937.2020.1839486.

Patel, V. K., Boudreaux, P. R., Gluesenkamp, K. R. 2021. "Validated Model of a Thermoelectric Heat Pump Clothes Dryer using Secondary Pumped Loops." *Applied Thermal Engineering*, vol. 184, 116345, https://doi.org/10.1016/j.applthermaleng.2020.116345.

Patel, V., Gluesenkamp, K. R., Goodman, D., Gehl, A. 2018. "Experimental Evaluation and Thermodynamic System Modeling of Thermoelectric Heat Pump Clothes Dryer." *Applied Energy*, vol. 217, 221–232, https://doi.org/10.1016/j.apenergy.2018.02.055.

5.2 CONFERENCE PAPERS

Gluesenkamp, K. R., Boudreaux, P., Shen, B., Goodman, D., Patel, V. K. 2018. "Experimental Measurements of Clothes Dryer Drum Heat and Mass Transfer Effectiveness." 5th International High Performance Buildings Conference, Purdue University, West Lafayette, IN, July 9–12.

Goodman, D. K., Patel, V. K., Gluesenkamp, K. R. 2017. "Thermoelectric Heat Pump Clothes Dryer Design Optimization." 12th IEA Heat Pump Conference 2017, Rotterdam, Netherlands, May 15–18.

Patel, V. K., Gluesenkamp, K. R. 2017. "Development of Packaging and Modular Control of Thermoelectric Clothes Dryer, With Performance Evaluation." ASME InterPACK 2017, Session 4-3-2, San Francisco, CA, August 29–September 1.

Patel, V. K., Gluesenkamp, K. R. 2018. "Thermoelectric Heat Pump Clothes Dryer using Secondary Loop Heat Exchangers: Experimental Evaluation." 5th International High Performance Buildings Conference, Purdue University, West Lafayette, IN, July 9–12.

Patel, V. K., Wang, H., Gluesenkamp, K. R., Gehl, A., Ormston, G., Kirkman, E. 2018. "Long-Term Effects of Power Quality and Power Cycling on Thermoelectric Module Performance." *Proceedings of the ASME 2018 International Technical Conference and Exhibition on Packaging and Integration* *of Electronic and Photonic Microsystems* (InterPACK), San Francisco, CA, August 28–30, V001T04A008.

Patel, V., Goodman, D., Gluesenkamp, K., Gehl, T. 2016. "Experimental Evaluation and Thermodynamic System Modeling of Thermoelectric Heat Pump Clothes Dryer." 16th Refrigeration and Air Conditioning Conference, Purdue University, West Lafayette, IN, July 11.

Shen, B., Gluesenkamp, K. R., Boudreaux, P., Patel, V. K. 2018. "Model-Based Air Flow Path Optimization for Heat Pump Clothes Dryer." 17th International Refrigeration and Air Conditioning Conference, Purdue University, West Lafayette, IN, July 9–12.

5.3 MAGAZINE ARTICLES

Nawaz, K., Gluesenkamp, K. R., Patel, V. K. 2020. "Heat Pump R&D for Appliance Applications." *Heat Pumping Technologies Magazine*, vol. 38, no. 1/2020, 4, ISSN 2002-018X.

5.4 PRESENTATIONS AND LECTURES

Gluesenkamp, K. R. 2018. "Thermoelectric Clothes Dryer." DOE Building Technologies Office 6th Annual Peer Review, Arlington, VA, April 30–May 3, https://www.energy.gov/sites/prod/files/2018/06/f52/32226o_Gluesenkamp_050218-1100.pdf.

6. CONCLUSIONS, COMMERCIALIZATION POSSIBILITIES, AND PLANS FOR FUTURE COLLABORATION

The following lessons were learned through this project developing a prototype TED:

1. When using TE modules to heat air entering the drum for tumble clothes drying, a suitable intermediate heat transfer mechanism is needed. For this work, both Al heat sinks and pumped water loops with water-to-air heat exchangers were investigated.

2. Pin-and-fin style heat sinks were investigated. Because of the large amount of Al expected, manufacturing costs are expected to be high, and manufacturing difficulties are expected because of the large number of mating surfaces. Furthermore, the heat sinks have a large pressure drop, requiring more energy to move air through the dryer airflow path than with typical tumble clothes dryers.

3. When using pumped water loops, the durability of the water loop components is critical to ensure no leaks occur. Plastic parts and Al are difficult to bond well in a durable manner.

4. Water-to-air HXs with as-low-as-possible pressure drop and predicted heat transfer increase the performance of TED when using a pumped water loop as the heat transfer mechanism between the TE modules and air.

5. Simple component swaps such as a more efficient blower and drum motor markedly increased performance, but these components are also more expensive than ones typically used in residential dryers.

6. Variations in current applied to the TE modules throughout the dry cycle affect the overall performance. Periods of lower current or short periods of no current can help increase performance, decreasing overall power consumption while negligibly affecting the dry time.

ORNL and CRADA partner Samsung Electronics America have developed an efficient prototype clothes dryer that uses TEHPs instead of electric resistance to dry the cloth load. The prototype fabricated at ORNL successfully demonstrated in the laboratory a CEF of 6.89 lb_c/kWh at standard conditions of 75°F and 50% relative humidity, exceeding the original project target of 6.0 lb_c/kWh. Additional trials on the same prototype achieved faster dry times with slightly lower CEFs, meeting all requirements for ENERGY STAR product qualification. Deploying dryers with CEFs of 6.0 lb_c/kWh nationwide represents a technical potential of 234 TBtu/year primary energy savings.

The work in this CRADA has led to follow-on projects on integration of thermoelectric heat pumps with dishwashers. A key advantage with dishwashers is the opportunity to provide a non-energy consumer benefit (better dish drying) in addition to the efficiency advantages.

7. ACKNOWLEDGMENTS

This work was sponsored by DOE's BTO under Contract No. DE-AC05-00OR22725 with UT-Battelle LLC. This research used resources at the Building Technologies Research and Integration Center, a DOE Office of Science user facility operated by ORNL.

The authors would like to acknowledge Tony Bouza, technology manager—HVAC and refrigeration, water heating, and appliances, DOE BTO. The authors would also like to acknowledge Steve Kowalski for critical review of the report, Emma Shamblin for technical editing, and Ayyoub Momen for program management.

8. REFERENCES

10 CFR Part 430. 2013. "Energy Conservation Program for Consumer Products." *Code of Federal Regulations*, Title 10, *Energy*, Part 430, Washington, DC.

DOE. 2016. *Building Technologies Office Multi-Year Program Plan: Fiscal Years 2016–2020*. Washington, DC: US Department of Energy Office of Energy Efficiency & Renewable Energy.

Patel, V., Gluesenkamp, K. R., Goodman, D., Gehl, A. 2018. "Experimental Evaluation and Thermodynamic System Modeling of Thermoelectric Heat Pump Clothes Dryer." *Applied Energy*, vol. 217, 221–232, https://doi.org/10.1016/j.apenergy.2018.02.055.